Available online at www.sciencedirect.com
SCIENCE DIRECT®
Polyhedron 25 (2006) 1771–1778
POLYHEDRON
www.elsevier.com/locate/poly

'Silver bullets' in antimicrobial chemotherapy: Synthesis, characterisation and biological screening of some new Ag(I)-containing imidazole complexes

Raymond Rowan [a], Theresa Tallon [a], Anita M. Sheahan [a], Robert Curran [a], Malachy McCann [a,*], Kevin Kavanagh [b], Michael Devereux [c], Vickie McKee [d]

[a] *Chemistry Department, National University of Ireland Maynooth, Maynooth, Co. Kildare, Ireland*
[b] *Biology Department, National University of Ireland Maynooth, Maynooth, Co. Kildare, Ireland*
[c] *Dublin Institute of Technology, Cathal Brugha Street, Dublin, Ireland*
[d] *Chemistry Department, Loughborough University, Loughborough, Leics., LE11 3TU, UK*

Received 27 September 2005; accepted 15 November 2005
Available online 27 December 2005

Abstract

Simple synthetic routes are given to the Ag(I) complexes, $[Ag_2(imH)_4](salH)_2$ (imH = imidazole; $salH_2$ = salicylic acid), $[Ag(MeNO_2imH)_2]ClO_4 \cdot nH_2O$ ($MeNO_2imH$ = 2-methyl-5-nitroimidazole; $n = 1, 3$), $[Ag(NO_2im)]$ (NO_2imH = 5-nitroimidazole) and [Ag(apim)]ClO_4 (apim = 1-(3-aminopropyl)imidazole). X-ray crystal structures of $[Ag_2(imH)_4](salH)_2$, $[Ag(MeNO_2imH)_2]ClO_4 \cdot H_2O$ and [Ag(apim)]ClO_4 were obtained. The new Ag(I) complexes and related known Ag(I) imidazolates were screened for their growth inhibitory effects (in vitro) against the pathogenic bacteria methicillin-resistant *Staphylococcus aureus* (*MRSA*) and *Escherichia coli* and also the fungal pathogen *Candida albicans*. $[Ag_2(imH)_4](salH)_2$, in comparison to the prescription drug silver sulfadiazine, had significantly better anti-bacterial qualities, whilst against the fungus *C. albicans* it was 47 times more potent than the marketed drug ketoconazole.

Keywords: Imidazoles; X-ray structures; Silver(I); Anti-fungal; Anti-bacterial

1. Introduction

With the ever-increasing problem of microbe resistance to current antimicrobial drugs, particularly antibiotics, there is an urgent demand for new classes of compounds that will efficiently inhibit the growth of pathogenic microorganisms. Silver and its simple salts have been known for centuries to exert anti-infective properties. However, the use of silver metal and its salts as antimicrobial agents declined sharply towards the middle of the last century upon the introduction of antibiotics. Amongst the few silver(I) compounds commonly prescribed today for their topical anti-bacterial effects are silver sulfadiazine (Silvadene®, Flamazine®) for the treatment of burns, and a dilute solution of $AgNO_3$, which is used for the prophylaxis of infectious bacterial conjunctivitis in infants [1,2]. Ag(I)-impreganted carboxymethylcellulose, marketed as 'Aquacel Ag', is a hydrofibre dressing with acclaimed antimicrobial properties and is prescribed for use on various categories of open wounds [3]. Along similar lines, Youngs et al. [4] recently reported the preparation of nano-fibre mats encapsulating an Ag(I)-imidazole cyclophane *gem*-diol complex and demonstrated the impressive bactericidal and fungicidal properties of the material. Biocide additives based on Ag(I) ions have been shown to exhibit an antimicrobial effect in various powder paint coating systems and are thought to have potential use in areas necessitating a sterile environment or where strict hygiene standards are required [5]. Silver sols (i.e., electrochemically generated colloidal suspensions of metallic silver in water) have also found application as bactericidal agents [6], although it has been

* Corresponding author. Tel.: +353 1 7083767; fax: +353 1 7083815.
E-mail address: malachy.mccann@nuim.ie (M. McCann).

0277-5387/$ - see front matter © 2005 Elsevier Ltd. All rights reserved.
doi:10.1016/j.poly.2005.11.021

recently reported [7] that such potency claims are misleading. The active agent is Ag^+, with bacterial metabolism being disrupted by its presence.

As part of our ongoing efforts into the development of new metal-based antimicrobial complexes [8–11] we have revisited the general area of silver-containing agents. Recently, a selection of mono- [12] and bi-nuclear [13] Ag(I) complexes, incorporating substituted imidazole ligands, were prepared and these displayed moderate activity against the human fungal pathogen *Candida albicans*. Imidazoles were selected as the coordinating ligands as these *N*-heterocycles bear a close relationship with naturally occurring biomolecules incorporating histidine residues. Although simple Ag(I) salts, such as $AgNO_3$ and $AgClO_4$, exhibit good anti-*Candida* activity (minimum inhibitory concentration (MIC) 30 and 44 μM, respectively, in RPMI media) this is surpassed by the salicylate complex $[Ag_2(salH)_2]$ ($salH_2$ = salicylic acid) (MIC = 5 μM in RPMI media) [14]. A further 10-fold enhancement in bioactivity was found for the ammonia-containing silver salicylate complex $[Ag_2(NH_3)_2(salH)_2]$ (MIC = 0.5 μM in RPMI media). Attempts to improve the antifungal activity by co-ligating salicylate with imidazole (imH = imidazole) at an Ag(I) centre forms the basis of the present work. Herein, is described the preparations of the Ag(I) complexes $[Ag_2(imH)_4](salH)_2$, $[Ag(MeNO_2imH)_2]ClO_4 \cdot nH_2O$ ($MeNO_2imH$ = 2-methyl-5-nitroimidazole; $n = 1$, 3), [Ag (NO_2im)] (NO_2imH = 5-nitroimidazole) and [Ag-(apim)]ClO_4 (apim = 1-(3-aminopropyl)imidazole). Ligand structures are shown in Fig. 1. X-ray crystal structures of $[Ag_2(imH)_4](salH)_2$, $[Ag(MeNO_2imH)_2]ClO_4 \cdot H_2O$ and [Ag(apim)]ClO_4 were obtained.

The new Ag(I) complexes, in addition to previously known and related Ag(I) imidazolates, were screened for their growth inhibitory effects (in vitro) against the following opportunistic human microbial pathogens: the Gram positive coccus bacterium methicillin-resistant *Staphylococcus aureus* (*MRSA*), the Gram negative bacillus bacterium *Escherichia coli* and the fungus *C. albicans*.

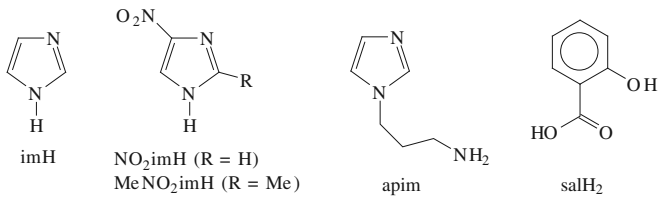

Fig. 1. Ligand structures and abbreviations.

2. Results and discussion

The imidazole/salicylate complex $[Ag_2(imH)_4](salH)_2$ forms in moderate yield by reacting $[Ag_2(salH)_4]$ with imidazole in an approximate 1:4 molar ratio (Scheme 1). The complex was characterised by X-ray crystallography (Fig. 2 and Table 1) and comprises a H-bonded supramolecular assembly. Two neutral imH ligands are bonded to the metal via their imine N atoms (mean Ag–N = 2.0951(15) Å) in an almost linear fashion (N3–Ag1–N1 = 178.82(6)°). There is a very weak Ag–Ag interaction (Ag···Ag = 3.7178(4) Å) but the more important contributions to holding the assembly together are the H-bonds involving the carboxylate oxygens of the $salH^-$ ligands and the H atom on the imidazole amine N atom. There are also π–π interactions between the imidazole rings (inclined at 16° to each other and, on average, the vertical distance between the rings is ca. 3.4 Å) and a further long interaction (2.9702(14) Å) between the Ag(I) centre and an adjacent phenolic oxygen atom (Fig. 3). The structure of $[Ag_2(imH)_4](salH)_2$ differs markedly from that of $[Ag_2(NH_3)_2(salH)_2]$ [14], where each metal is coordinated directly to a salicylate carboxylate oxygen (Ag–O = 2.1699(14) Å) and to an ammonia nitrogen atom (Ag–N = 2.1367(17) Å), and also in a slightly less linear manner {O3–Ag–N1 = 175.37(5)°}. In addition, the Ag–Ag distance in $[Ag_2(NH_3)_2(salH)_2]$ (3.0685(4) Å) is significantly shorter than in $[Ag_2(imH)_4](salH)_2$. Gold and Gregor [15] calculated the formation constants (in aqueous 1.0 M KNO_3) for $[Ag(imH)]^+$ ($\log K_1 = 3.11$) and $[Ag(imH)_2]^+$ ($\log K_2 = 3.73$) to be very similar to those for $[Ag(NH_3)]^+$ and $[Ag(NH_3)_2]^+$ ($\log K_1 = 3.24$, $\log K_2 = 3.81$).

A brief comment on the synthesis and structures of other related Ag(I) complexes containing non-functionalised imidazole ligands is warranted. The imidazole complex salt $[Ag(imH)_2]NO_3$ has been prepared by reacting $AgNO_3$ with imH (ca. 1:4 molar ratio) [16] and in the $[Ag(imH)_2]^+$ cation the metal is bonded to the imine N atoms of two neutral imidazole ligands [17] and in a similar fashion to that found in the core structure of $[Ag_2(imH)_4](salH)_2$. In $[Ag(imH)_2]^+$ the two Ag–N bonds lie 5.7° and 3.2° out of the imidazole planes, respectively, and the dihedral angle between the imidazole groups is 20.2°. $[Ag(imH)_2]NO_3$ forms at pH ~4, suggesting that Ag(I) ions compete against protons for imidazole groups more successfully than for amino groups. Amines are, in fact, much stronger bases than imidazole towards protons [17]. The imidazolate complex, [Ag(im)], containing a deprotonated imidazole (im^-) ligand, has been prepared in a similar manner to $[Ag(imH)_2]NO_3$, but with the inclusion of NaOH in the

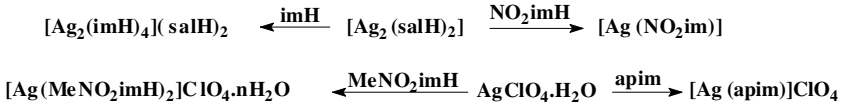

Scheme 1.

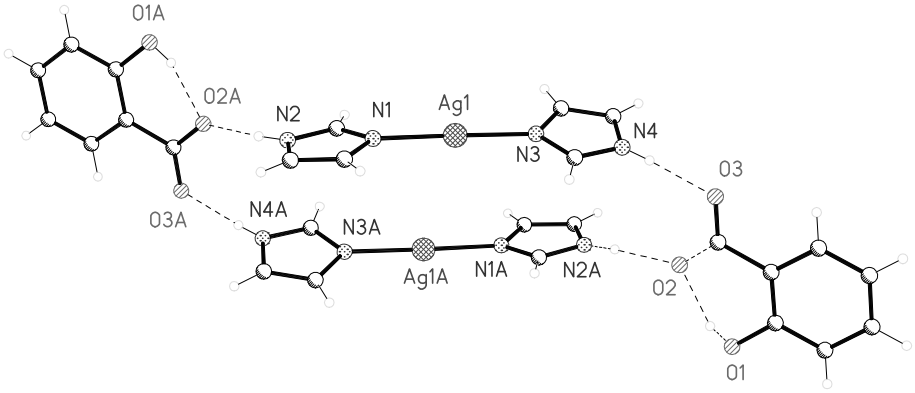

Fig. 2. Structure of $[Ag_2(imH)_4](salH)_2$.

Table 1
Selected bond lengths (Å) and angles (°) for $[Ag_2(imH)_4](salH)_2$

Ag(1)–N(3)	2.0934(15)
Ag(1)–N(1)	2.0967(15)
Ag(1)–O(1)#1	2.9702(14)
Ag(1)–Ag(1)#2	3.7178(4)
N(3)–Ag(1)–N(1)	178.82(6)
N(3)–Ag(1)–O(1)#1	98.67(5)
N(1)–Ag(1)–O(1)#1	81.63(5)
N(3)–Ag(1)–Ag(1)#2	96.90(4)
N(1)–Ag(1)–Ag(1)#2	82.09(4)
O(1)#1–Ag(1)–Ag(1)#2	133.03(3)

Symmetry transformations used to generate equivalent atoms: #1 x, y, $z-1$; #2 $-x+1$, $-y$, $-z+1$.

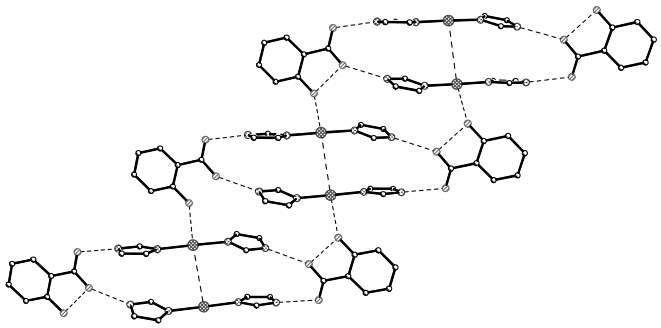

Fig. 3. Interaction between the Ag(I) centre and an adjacent phenolic oxygen atom in the structure of $[Ag_2(imH)_4](salH)_2$.

reaction mixture [16,18]. Ionisation of imH to im^- changes the monodentate imH lig into the bifunctional im^- ligand and X-ray powder diffraction studies [18] have revealed the polymeric nature of [Ag(im)] (mean Ag–N 2.08 Å) with linearly coordinated N–Ag–N ligands (171.8(8)° and 167.6(1)°) and short interchain Ag···Ag contacts (3.161(4) Å). Hexameric $[Ag_6(imH)_{12}](ClO_4)_6$ forms from $AgClO_4$ and imH in water containing added perchloric acid [19] and the large cation comprises a planar $(Ag^+)_6$ cluster, in which three radiating pairs of Ag^+ ions (3.051(1) Å apart) are on the corners of an equilateral triangle, the inner Ag^+ ions being 3.493(1) Å apart. Each metal ion carries two, linearly coordinated, neutral imidazole ligands and two distinct Ag–N bonding distances are evident (Ag(1)–N(1) 2.075(3) Å; Ag(2)–N(3) 2.089(3) Å).

Reaction of $MeNO_2imH$ with $AgClO_4$ in a 2:1 molar ratio gives $[Ag(MeNO_2imH)_2]ClO_4 \cdot 3H_2O$ in good yield (Scheme 1). Initial attempts to form an Ag(I) complex of $MeNO_2imH$ by reaction with $AgClO_4$ in a 4:1 molar ratio led to the co-crystallisation of metal-free $MeNO_2imH$ with $[Ag(MeNO_2imH)_2]ClO_4 \cdot H_2O$. This Ag(I) monohydrate complex was crystallographically characterised (Fig. 4 and Table 2) (orthorhombic, *Pnma*). The metal ion lies on a centre of symmetry and the perchlorate anion rests on a mirror plane, such that the asymmetric unit comprises half of the cation, half the anion and one water molecule. The metal ion is bonded to the imine N atoms (adjacent to the nitro group) of two diagonally opposed $MeNO_2imH$ ligands (Ag–N = 2.126(0) Å; N–Ag–N = 180°). There are also long intramolecular contacts between one nitro O

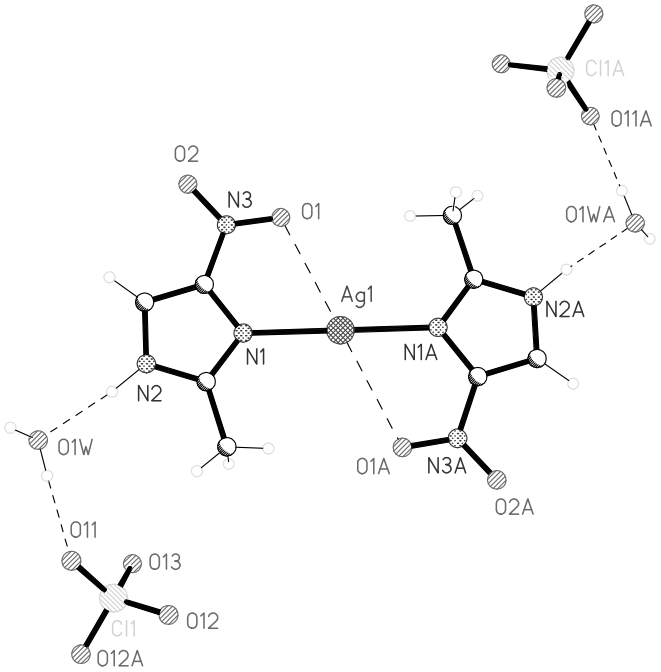

Fig. 4. Structure of $[Ag(MeNO_2imH)_2]ClO_4 \cdot H_2O$.

Table 2
Selected bond lengths (Å) and angles (°) for $[Ag(MeNO_2imH)_2]ClO_4 \cdot H_2O$

Ag(1)–N(1)	2.1260(16)
Ag(1)–O(2)#1	2.8735(17)
Ag(1)–O(1)	2.9236(17)
N(3)–O(1)	1.231(2)
N(3)–O(2)	1.234(2)
N(1)#2–Ag(1)–N(1)	180.0
N(1)#2–Ag(1)–O(2)#1	94.29(5)
N(1)–Ag(1)–O(2)#1	85.71(5)
N(1)#2–Ag(1)–O(1)	115.75(5)
N(1)–Ag(1)–O(1)	64.25(5)
O(2)#1–Ag(1)–O(1)	115.85(5)

Symmetry transformations used to generate equivalent atoms: #1 $x - 1/2$, y, $-z + 1/2$; #2 $-x + 2$, $-y + 1$, $-z$.

atom on each $MeNO_2imH$ ligand and the metal (Ag1–O1 = 2.9236(17) Å; O1A–Ag–O1 = 180°). The $[Ag(MeNO_2imH)_2]^+$ cations are linked into two-dimensional sheets via shorter ONO–Ag–ONO axial interactions (Ag1–O2#1 = 2.8735(17) Å) (Fig. 5) and these, in turn, are linked by hydrogen-bonding through the water solvate, to intervening layers containing the perchlorate anion and water molecule. As a consequence of the inter- and intramolecular ONO–Ag interactions the nitrate N–O distances in $[Ag(MeNO_2imH)_2]ClO_4 \cdot H_2O$ are marginally longer than in metal-free $MeNO_2imH$ [20].

The related, non-methylated imidazole, 5-nitroimidazole (NO_2imH), is known to react with $AgNO_3$ and $AgBF_4$ in strongly acidic solution to form the salts $[Ag(NO_2imH)_2]X$

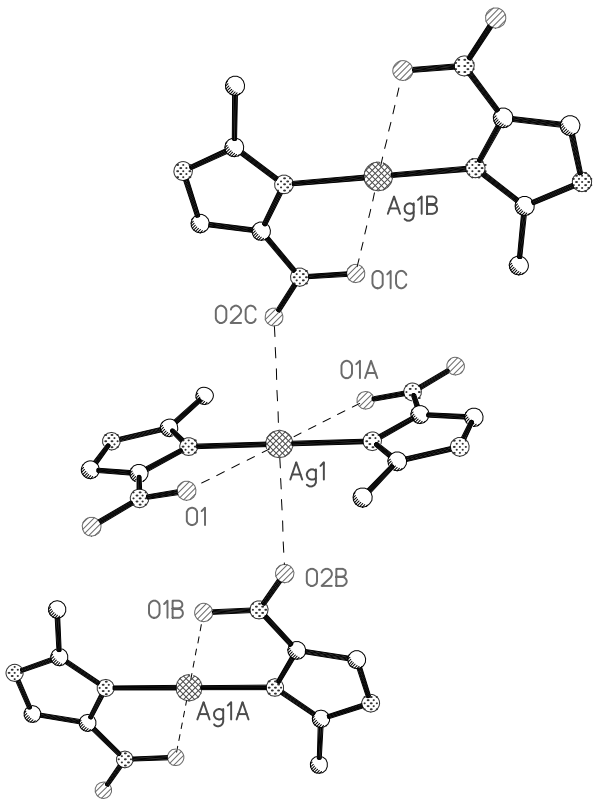

Fig. 5. Linking of $[Ag(MeNO_2imH)_2]^+$ cations into two-dimensional sheets via long Ag–ONO interactions.

($X = NO_3$, BF_4) [21]. Both salts have been crystallographically characterised ($[Ag(NO_2imH)_2]NO_3$, monoclinic, $P2/n$; $[Ag(NO_2imH)_2]BF_4$, monoclinic, $P2_1/c$), and in each case the metal is coordinated to the endocyclic N atom adjacent to the nitro group (mean N–Ag–N = 166.1° for nitrate salt and 175.2° for tetrafluoroborate salt). One O atom of each nitro group makes a secondary Ag–O bond near the equatorial plane. The anions are hydrogen bonded to the ligand NH groups. Whilst the mean Ag–N and Ag–O bonding distances in $[Ag(NO_2imH)_2]X$ and $[Ag(MeNO_2imH)_2]ClO_4 \cdot H_2O$ are quite similar substantial differences are apparent in the N–Ag–N, O–Ag–O and N–Ag–O bond angles. Solution ^1H and ^{13}C NMR spectra of the $[Ag(NO_2imH)_2]X$ salts showed that the cationic complexes dissociate in DMSO [21].

It was also reported [21] that in neutral or weakly acidic aqueous media NO_2imH reacts with $AgNO_3$ and $AgBF_4$ to give the insoluble NO_2im^- complex, $[Ag(NO_2im)]$, whose IR and ^{13}C NMR spectra were consistent with a polymeric chain of deprotonated ligands bridging Ag(I) centres via the ring N atoms. In the present work the related complex, $[Ag(MeNO_2im)]$, is obtained upon addition of $MeNO_2imH$ to $[Ag_2(salH)_4]$ in a 3:1 molar ratio (Scheme 1), suggesting that deprotonation of $MeNO_2imH$ is a consequence of the basicity of the $salH^-$ ion (pK_a of $salH_2 = 3.4$).

The white solid, $[Ag(apim)]ClO_4$, forms in good yield upon treating $AgClO_4$ with apim in ethanol (Scheme 1). The insolubility of the complex (in ethanol and water) suggested a polymeric structure involving the primary amine group and the ring imine N atom. This was confirmed by X-ray crystallographic studies (Figs. 6 and 7; Table 3) which revealed a wavy polymeric chain containing two-coordinate Ag(I) ions with additional weaker metal-perchlorate Ag–ClO_4–Ag intrastrand interactions. Each perchlorate also makes two further interstrand H-bonds to amine protons (not shown in figures). Furthermore, there are interstrand crosslinks arising from weak Ag–N(imine) interactions (Fig. 7). There are also very weak interactions between perchlorate ions and imine nitrogens (not shown in figures) but there are no indications of any significant Ag–Ag bonding.

Microbial growth inhibition data are given in Table 4. The metal-free organic ligands were essentially inactive against all of the test microbes. All of the tabulated silver-containing species exhibited significantly greater anti-fungal than anti-bacterial activity. $[Ag_2(imH)_4](salH)_2$ was, universally, the most active complex. The complex, in comparison to the prescription drug silver sulfadiazine, had significantly better anti-bacterial qualities, whilst against the fungus *C. albicans* it was 47 times more potent than the marketed drug ketoconazole. Surprisingly, the hexanuclear imidazole complex, $[Ag_6(imH)_{12}](ClO_4)_6$, was ineffective against both bacterial species but was highly toxic towards *C. albicans*, indicating some degree of selectivity between anti-bacterial and anti-fungal activity. In a similar fashion, the simple Ag(I) salts, $AgNO_3$ and $AgClO_4 \cdot H_2O$, and the nitroimidazolate complex, $[Ag(NO_2im)]$, were only marginally active against bacteria

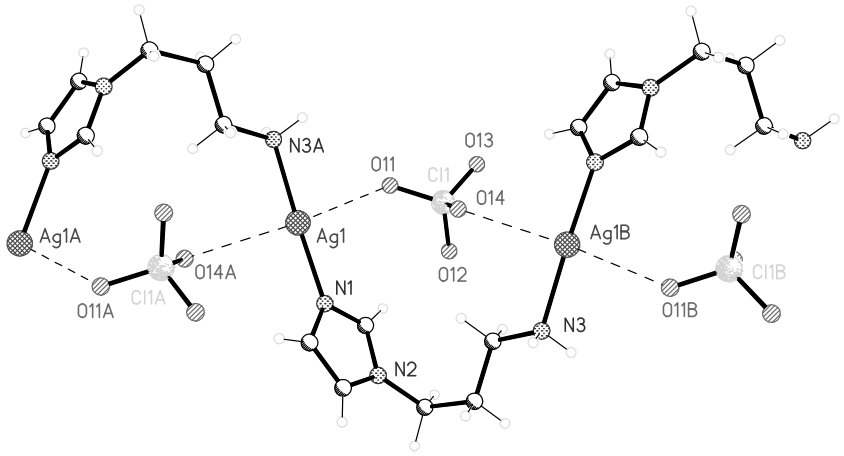

Fig. 6. Section of the structure of polymeric Ag(apim)]ClO_4.

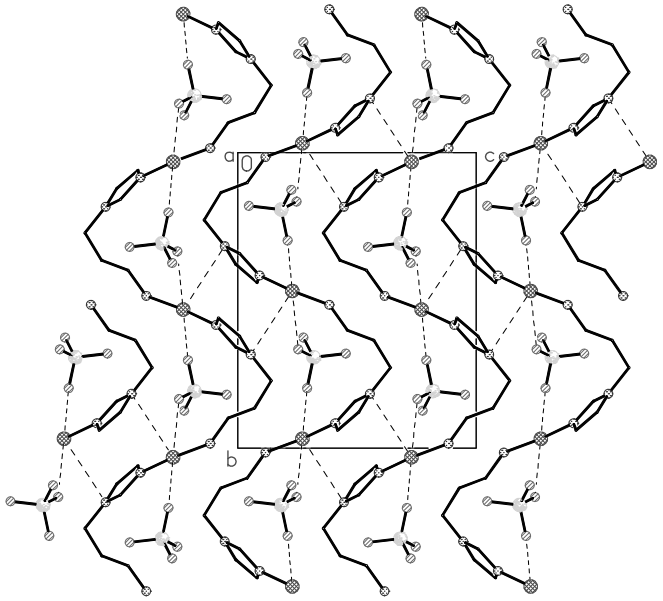

Fig. 7. Alignment of polymer chains in the structure of [Ag(apim)]ClO_4.

Table 3
Selected bond lengths (Å) and angles (°) for [Ag(apim)]ClO_4

Ag(1)–N(1)	2.1004(17)
Ag(1)–N(3)#1	2.1374(17)
Ag(1)–O(11)	2.9269(18)
Ag(1)–O(14)#1	3.1368(19)
N(3)–Ag(1)#2	2.1374(17)
N(1)–Ag(1)–N(3)#1	173.56(6)
N(1)–Ag(1)–O(11)	97.40(6)
N(3)#1–Ag(1)–O(11)	83.79(6)
N(1)–Ag(1)–O(14)#1	87.05(6)
N(3)#1–Ag(1)–O(14)#1	92.16(5)
O(11)–Ag(1)–O(14)#1	174.47(5)

Symmetry transformations used to generate equivalent atoms: #1 $-x$, $y+1/2$, $-z+1/2$; #2 $-x$, $y-1/2$, $-z+1/2$.

Table 4
Antimicrobial activity

Complex	MRSA, MIC_{50} (μM)	*E. coli*, MIC_{50} (μM)	*C. albicans*, MIC_{100} (μM)
imH	≫50	≫50	≫50
NO_2imH	≫50	≫50	≫50
$MeNO_2$imH	≫50	≫50	≫50
apim	≫50	≫50	≫50
$salH_2$	≫50	≫50	≫50
Ketoconazole			4.7
Silver sulfadiazine	19.6	14.0	3.5
$AgNO_3$	36.8	35.3	1.8
$AgClO_4 \cdot H_2O$	43.4	48.2	1.4
$[Ag_2(imH)_4](salH)_2$	10.5	10.5	0.1
$[Ag(MeNO_2imH)_2]ClO_4 \cdot 3H_2O$	15.5	15.5	4.8
[Ag(apim)]ClO_4	30.1	30.1	1.8
[Ag(NO_2im)]	45.5	54.6	2.8
$[Ag_2(salH)_2]$	40.8	42.8	0.6
$[Ag_2(salH)_2(NH_3)_2]$	17.2	19.1	0.6
$[Ag_6(imH)_{12}](ClO_4)_6$	≫50	≫50	0.3

but quite effective against the fungal species. Whilst $[Ag_2(salH)_2]$ and $[Ag_2(salH)_2(NH_3)_2]$ also exhibited a toxicity bias towards *C. albicans*[1] the ammonia-containing adduct was more than twice as potent towards both bacterial species. $[Ag(MeNO_2imH)_2]ClO_4 \cdot 3H_2O$ and silver sulfadiazine displayed similar bacterial and fungal activities.

In relation to bacteria, it is important to note that morphological changes have been reported [22] to occur in $AgNO_3$-treated *S. aureus* and *E. coli* cells. Transformations included shrinkage of the cytoplasmic membrane, possible detachment of the membrane from the cell wall and DNA condensation coupled with a loss of replication. In addition to these morphological changes, protein conglomeration also occurred in response to $AgNO_3$ treatment, and it was postulated that this event was possibly to protect the cell from DNA damage. Furthermore, it was suggested that the higher dose of $AgNO_3$ was required to kill Gram

[1] In the current work, $[Ag_2(salH)_2]$ and $[Ag_2(NH_3)_2(salH)_2]$ are equally effective against *C. albicans* in minimal media. However, in RPMI media $[Ag_2(NH_3)_2(salH)_2]$ displays approximately 10-fold superior activity than $[Ag_2(salH)_2]$ (see Ref. [17]).

positive (*S. aureus*) than Gram negative (*E. coli*) cells reflected the fact that the cell wall of the latter species was considerably thinner. In contrast, under the experimental conditions in which the present study was conducted, neither the Ag(I) complexes or the simple Ag(I) salts discriminated markedly in their activities towards Gram positive (MRSA) and Gram negative bacteria (*E. coli*).

3. Experimental

Chemicals were purchased from commercial sources and, unless specified, were used without further purification. Literature methods were used to make $[Ag_2(salH)_2]$ [23–25], $[Ag_2(NH_3)_2(salH)_2]$ [14] and [Ag(im)] [17,19]. Preparations of silver complexes were conducted in the absence of light and the samples were stored in the dark. Infrared spectra of solids (in a KBr matrix) were recorded in the region 4000–400 cm^{-1} on a Nicolet FT-IR Impact 400D infrared spectrometer. Microanalytical data were provided by the Microanalytical Laboratory, National University of Ireland, Cork, Ireland.

Candida albicans (ATCC 10231, Manasas, VA, USA) was grown on Sabouraud dextrose agar (SDA) plates at 37 °C and maintained at 4 °C for short-term storage. Cultures were routinely sub-cultured every 4–6 weeks. Cultures were grown to the stationary phase (approximately 1×10^8 cells cm^{-3}) overnight at 37 °C and 200 rpm in minimal medium (2% w/v glucose, 0.5% w/v yeast nitrogen base (without amino acids or ammonium sulfate), 0.5% w/v ammonium sulfate), again at 37 °C. Solutions of water-soluble test compounds were prepared by dissolving the compound (0.02 g) in distilled water (10 cm^3) to yield a stock solution with a concentration of 2000 μg cm^{-3}. Complexes which were insoluble in both water and DMSO were made up (with vigorous agitation) as suspensions in water to give stock suspensions of 2000 μg cm^{-3}. Complexes which were insoluble in water, but soluble in DMSO, were dissolved (0.02 g) in DMSO (1 cm^3) and added to water (9 cm^3) to give a stock solution (concentration 2000 μg cm^{-3}). Doubling dilutions of these various stock solutions (or suspensions) were made to yield a series of test solutions (or suspensions). It is important to note that, in general, the antimicrobial activity of the Ag-containing solutions/suspensions deteriorated markedly even upon storage at 4 °C for short periods. Thus, fresh solutions/suspensions were prepared immediately prior to testing. Minimum inhibitory concentrations (MIC_{100} values, minimum concentration required to inhibit 100% of cell growth) were then determined using the broth microdilution method [26,27].

Escherichia coli was obtained from the Clinical Microbiology Laboratory, St. James's Hospital, Dublin, Ireland, and MRSA from Microbiologics, North St. Cloud Mn, USA. Bacteria were maintained on Nutrient Agar plates at 4 °C and cultured in liquid broth (LB) when required. LB was used for the antibacterial testing. LB (13 g) was dissolved in water (1 L) in a Duran bottle, and then dispensed into 250 cm^3 conical flasks, autoclaved and allowed to cool. Both *E. coli* and MRSA were grown in LB at 30 °C and 200 rpm to an OD_{600} of 1.0. A microtiter plate was inoculated with 100 μl of bacterial cells ($OD_{600} = 1.0$). Solutions of silver complexes were prepared by dissolving (or suspending) the complex (0.02 g) in DMSO (0.5 cm^3). To this solution/suspension was added filter-sterilised Millipore water (9.5 cm^3) to produce a stock solution/suspension of concentration 2000 μg cm^{-3}. Stock solution/suspension (1.0 cm^3) was added to nutrient broth media (9 cm^3) to produce a drug solution/suspension of concentration 200 μg cm^{-3} with the concentration of DMSO being 0.5%. This solution/suspension (100 μl) was added to the microtiter plate. 1:1 serial dilutions were made so as to produce a test concentration range of 50–0.1 μg cm^{-3}. The plates were incubated at 30 °C overnight and OD_{600} values were read using an RMX plate reader (USA) to give MIC_{50} values (minimum concentration required to inhibit 50% of cell growth). Experiments were performed in triplicate and the data analysed using MICROSOFT EXCEL.

3.1. $[Ag_2(imH)_4](salH)_2$

$[Ag_2(salH)_2]$ (0.37 g, 0.76 mmol) and imidazole (0.23 g, 3.38 mmol) were refluxed in ethanol (15 cm^3) for 2.5 h. The mixture was filtered whilst hot to remove a small amount of a pale pink solid. The filtrate was concentrated to dryness to give a white solid product. The solid was washed with ethanol and allowed to air-dry. Yield: 0.30 g (52%). To obtain crystals suitable for X-ray structural analysis the original filtrate was allowed to slowly evaporate to low volume over a period of days. The white complex was only soluble in warm DMSO. *Anal.* Calc.: C, 40.96; H, 3.44; N, 14.70. Found: C, 40.64; H, 3.30; N, 14.03%. IR: 3419, 1608, 1486, 1377, 1062, 745 cm^{-1}.

3.2. $[Ag(apim)]ClO_4$

$AgClO_4$ (0.5 g, 2.2 mmol) was dissolved in ethanol (20 cm^3) and apim (0.69 g, 5.5 mmol) added. The resulting white suspension was stirred at room temperature for 1 h and the solvent then decanted off. The solid was washed with ethanol (3×10 cm^3) and then dried under vacuum. Yield: 0.58 g (72%). The complex was only very slightly soluble in DMSO and insoluble in all other solvents. *Anal.* Calc.: C, 21.67; H, 3.33; N, 12.64. Found: C, 22.57; H, 3.36; N, 13.04%. IR: 3323, 3110, 2935, 1511, 1111, 1088, 627 cm^{-1}.

3.3. $[Ag(MeNO_2imH)_2]ClO_4 \cdot 3H_2O$

To a solution of 2-methyl-5-nitroimidazole (0.224 g, 1.76 mmol) in ethanol (20 cm^3) was added silver prechlorate monohydrate (0.215 g, 0.95 mmol) and the reaction mixture refluxed for 2 h. A small amount of an insoluble white solid was filtered off and the filtrate concentrated to give the product as a white powder. The solid was washed with water and then with ethanol and then air-dried. Yield: 0.36 g (76%).

The complex was reasonably stable in light and was sparingly soluble in DMSO and insoluble in all other common solvents. *Anal*. Calc.: C, 18.64; H, 3.13; N, 16.30. Found: C, 18.63, H, 2.27, N, 16.00%. IR: 3162, 3045, 2896, 1711, 1572, 1506, 1380, 1286, 1103, 815, 752, 627 cm^{-1}.

3.4. $[Ag(MeNO_2imH)_2]ClO_4 \cdot H_2O$

Crystals of composition $[Ag(MeNO_2imH)_2]ClO_4 \cdot H_2O$ co-crystallised with some unreacted 2-methyl-5-nitroimidazole when 2-methyl-5-nitroimidazole was reacted with silver prechlorate monohydrate in a 4:1 molar ratio and following the procedure outlined for the above preparation of $[Ag(MeNO_2imH)_2]ClO_4 \cdot 3H_2O$.

3.5. $[Ag(NO_2im)]$

$[Ag_2(salH)_2]$ (0.40 g, 0.82 mmol) and 5-nitroimidazole (0.28 g, 2.48 mmol) were refluxed in ethanol (20 cm^3) for 1 h. The resulting white suspension was filtered whilst hot and the solid washed with ethanol and then air-dried. Yield: 0.34 g (95%). The solid was insoluble in all common solvents. *Anal*. Calc.: C, 16.38; H, 0.92; N, 19.11. Found: C, 16.99; H, 0.74; N, 18.65%. IR: 3139, 1498, 1450, 1375, 1239, 1203, 1021, 821, 750, 659 cm^{-1}.

3.6. $[Ag_6(imH)_{12}](ClO_4)_6$

This complex was prepared using a modification of the literature method [19]. $AgClO_4$ (0.50 g, 2.41 mmol) was dissolved in H_2O (4 cm^3) and to this was added a solution of imidazole (0.30 g, 4.41 mmol) in H_2O (2 cm^3). To the resulting white suspension was added, dropwise, perchloric acid (1.5 cm^3) causing the white solid to dissolve. Ethanol (1.5 cm^3) was added and the solution was then concentrated to dryness under high vacuum. The majority of the white solid was redissolved in hot ethanol (20 cm^3). The mixture was filtered and ethyl acetate (25 cm^3) added to the filtrate. Solid $NaHCO_3$ was added portion-wise to the solution until CO_2 evolution ceased. After filtration, the filtrate was stirred for 0.5 h and then concentrated to dryness under high vacuum. The resulting white solid was re-suspended in ethyl acetate (40 cm^3) and then filtered off. The solid was washed with ethyl acetate (3×10 cm^3) and then air-dried. Yield: 0.34 g (45%). The complex was soluble in DMSO but insoluble in H_2O and EtOH.

3.7. X-ray crystallography

All data were collected at 150 K on a Bruker SMART 1000 CCD diffractometer using Mo Kα radiation ($\lambda = 0.71073$ Å) and the structures were solved by direct methods and refined by full-matrix least-squares on F^2 using all the data [28]. All non-hydrogen atoms were refined with anisotropic atomic displacement parameters and the hydrogen atoms bonded to carbon or amine nitrogen atoms were inserted at calculated positions using a riding model. Hydrogen atoms bonded to either oxygen or imidazole nitrogen atoms were located from difference maps and assigned common fixed isotropic displacement parameters; their coordinates were refined in $[Ag_2(imH)_4](salH)_2$ but not refined in $[Ag(MeNO_2imH)_2]ClO_4 \cdot H_2O$. Data collection and refinement parameters are summarised in Table 5.

Table 5
X-ray data for $[Ag_2(imH)_4](salH)_2$, $[Ag(MeNO_2imH)_2]ClO_4 \cdot H_2O$ and $[Ag(apim)]ClO_4$

Complex	$[Ag_2(imH)_4](salH)_2$	$[Ag(MeNO_2imH)_2]ClO_4 \cdot H_2O$	$[Ag(apim)]ClO_4$
Empirical formula	$C_{26}H_{26}Ag_2N_8O_6$	$C_8H_{12}AgClN_6O_9$	$C_6H_{11}AgClN_3O_4$
Crystal system	triclinic	orthorhombic	monoclinic
Space group	$P\bar{1}$	*Pnma*	$P2_1/c$
Cell dimensions			
a (Å)	8.6892(7)	11.7774(8)	7.7252(8)
b (Å)	9.1981(8)	25.1672(18)	12.9936(13)
c (Å)	9.7645(8)	5.3466(4)	10.4871(10)
α (°)	89.946(10)	90	90
β (°)	87.238(1)	90	91.425(2)
γ (°)	62.150(1)	90	90
Volume (Å^3)	689.02(10)	1584.8(2)	1052.35(18)
Z	2	4	4
Absolute coefficient (mm^{-1})	1.478	1.501	2.168
Crystal size (mm^3)	$0.41 \times 0.22 \times 0.13$	$0.23 \times 0.20 \times 0.13$	$0.48 \times 0.15 \times 0.09$
Crystal description	colourless block	colourless hexagonal prism	colourless flake
Reflections collected	5946	12 508	8709
Independent reflections (R_{int})	3113 (0.0104)	1961 (0.0227)	2431 (0.0161)
Completeness ($\theta = 25°$) (%)	99.4	100.0	100.0
Absorption correction	multi-scan	multi-scan	multi-scan
Data/restraints/parameters	3113/0/199	1961/0/122	2431/0/136
Goodness-of-fit on F^2	1.063	1.026	1.067
Final R_1, wR_2 [$I > 2\sigma(I)$]	0.0193, 0.0474	0.0218, 0.0475	0.0191, 0.0427
R_1, wR_2 (all data)	0.0217, 0.0484	0.0336, 0.0519	0.0232, 0.0441

4. Supplementary data

X-ray supplementary data for $[Ag_2(imH)_4](salH)_2$, $[Ag(MeNO_2imH)_2]ClO_4 \cdot 2H_2O$ and $[Ag(apim)]ClO_4$ are available from the Cambridge Crystallographic Data Centre, 12 Union Road, Cambridge CB2 1EZ, England, www.ccdc.cam.ac.uk/conts/retrieving.html (fax: +44 1223 336033 or e-mail: deposit@ccdc.cam.ac.uk), quoting the deposition numbers CCDC 272997, CCDC 272998 and CCDC 281737, respectively.

Acknowledgements

Financial support from the Higher Education Authority of Ireland through the Programme for Research in Third Level Institutions (R. Rowan) and from Kildare County Council, Ireland (T. Tallon) is gratefully acknowledged.

References

[1] J.M.T. Hamilton-Miller, S. Shah, Int. J. Antimicrob. Agent 7 (1996) 97.
[2] H.J. Klasen, Burns 26 (2000) 131.
[3] 'Aquacel Ag' Hydrofibre Dressing with Silver, E.R. Squibb & Sons, L.L.C., 2003.
[4] A. Melaiye, Z. Sun, K. Hindi, A. Milsted, D. Ely, D.H. Reneker, C.A. Tessier, W.J. Youngs, J. Am. Chem. Soc. 127 (2005) 2285.
[5] S. Zeren, A. Preuss, B. König, Paint Coat. Industry (April) (2005) 38.
[6] C.E. Housecroft, A.G. Sharpe, Inorganic Chemistry, Prentice-Hall, Gosport, 2001, p. 577.
[7] P. van Hasselt, B.A. Gashe, J. Ahmad, J. Wound Care 13 (2004) 154.
[8] M. Geraghty, J.F. Cronim, M. Devereux, M. McCann, BioMetals 13 (2000) 1.
[9] M. Devereux, M. McCann, V. Leon, R. Kelly, D. O'Shea, V. McKee, Polyhedron 22 (2003) 3187.
[10] B. Coyle, P. Kinsella, M. McCann, M. Devereux, R. O'Connor, M. Clynes, K. Kavanagh, Tox. in Vitro 18 (2004) 63.
[11] A. Eshwika, B. Coyle, M. Devereux, M. McCann, K. Kavanagh, BioMetals 17 (2004) 415.
[12] M. McCann, B. Coyle, J. Briody, F. Bass, N. O'Gorman, M. Devereux, K. Kavanagh, V. McKee, Polyhedron 22 (2003) 1595.
[13] S. Abuskhuna, J. Briody, M. McCann, M. Devereux, K. Kavanagh, J. Barreira Fontecha, V. McKee, Polyhedron 23 (2004) 1249.
[14] B. Coyle, M. McCann, K. Kavanagh, M. Devereux, V. McKee, N. Kayal, D. Egan, C. Deegan, G.J. Finn, J. Inorg. Biochem. 98 (2004) 1361.
[15] D.H. Gold, H.P. Gregor, J. Phys. Chem. 64 (1960) 1461.
[16] J.E. Bauman Jr., J.C. Wang, Inorg. Chem. 3 (1964) 368.
[17] C.B. Acland, H.C. Freeman, J. Chem. Soc., Chem. Commun. (1971) 1016.
[18] N. Masciocchi, M. Moret, P. Cairati, A. Sironi, G.A. Ardizzoia, G. La Monica, J. Chem. Soc., Dalton Trans. (1995) 1671.
[19] G.W. Eastland, M.A. Mazid, D.R. Russell, M.C.R. Symons, J. Chem. Soc., Dalton Trans. (1980) 1682.
[20] I. Ségalas, J. Poitras, A.L. Beauchamp, Acta Crystallogr. C: Cryst. Struct. Commun. C48 (1992) 295.
[21] I. Ségalas, A.L. Beauchamp, Can. J. Chem. 70 (1992) 943.
[22] Q.L. Feng, J. Wu, G.Q. Chen, F.Z. Cui, T.N. Kim, J.O. Kim, J. Biomed. Mater. Res. 52 (2000) 662.
[23] T.C.W. Mak, W.-H. Yip, C.H.L. Kennard, G. Smith, E.J. O'Reilly, Aust. J. Chem. 39 (1986) 541.
[24] G. Smith, C.H.L. Kennard, T.C.W. Mak, Z. Kristallogr. 184 (1988) 275.
[25] G.L. Maurer, V.E. Stephanini, Patent 4,278610 United States, 1981.
[26] M. McCann, M. Geraghty, M. Devereux, D. O'Shea, J. Mason, L. O'Sullivan, Metal Drug 7 (2000) 185.
[27] B. Coyle, K. Kavanagh, M. McCann, M. Devereux, M. Geraghty, BioMetals 16 (2003) 321.
[28] G.M. Sheldrick, SHELXTL Version 6.12, Bruker-AXS, Madison, WI, 2001.